

Received November 13, 2017, accepted December 25, 2017, date of publication December 29, 2017, date of current version March 9, 2018.

Digital Object Identifier 10.1109/ACCESS.2017.2788008

A Design of Broadband Circularly Polarized C-Shaped Slot Antenna With Sword-Shaped Radiator and Its Array for L/S-Band Applications

RUI XU¹, JIAN-YING LI, (Member, IEEE), AND JIE LIU

School of Electronics and Information, Northwestern Polytechnical University, Xi'an 710072, China

Corresponding author: Rui Xu (rxulj@163.com)

This work was supported by the National Natural Science Foundation of China under Grant 61271416 and Grant 61301093.

ABSTRACT In this paper, a novel wideband circularly polarized (CP) slot antenna and its array are presented. The antenna element consists of a C-shaped slot and a 50- Ω microstrip-fed port to achieve left-hand circular polarization. Both the impedance bandwidth (IBW) and the 3-dB axial ratio bandwidth (ARBW) are greatly broadened by off-center microstrip-fed sword-shaped structure. A 2×2 array prototype based on the proposed CP element is also designed. Sequential rotation microstrip-feeding structure is used to excite four antennas and to realize good symmetric unidirectional radiation. To verify this design, both the CP antenna element and 2×2 array are fabricated and measured. The measured results of the antenna element exhibit an IBW of 132% (0.85–4.15 GHz) and an ARBW of 95.7% (1.20–3.40 GHz). The measured ARBW and IBW of the 2×2 antenna array are about 108.3% (1.10–3.70 GHz) and 100% (1.15–3.45 GHz), respectively. And the measured peak gain of the antenna array reaches 13.4 dBic. The proposed antenna is very suitable for CP applications in L/S bands.

INDEX TERMS Circularly polarized, broadband, C-shaped slot, antenna array.

I. INTRODUCTION

With the rapid development of modern wireless communication system, the circularly polarized (CP) antenna has gained more and more attention due to its advantages of reducing multipath interference. CP antennas have been widely used in wireless local area networks (WLANs), radio frequency identification devices (RFIDs), and many other communication systems. Due to the high Q value, traditional single-feed microstrip CP antennas [1], [2] have a very narrow impedance and AR bandwidth. A communication system that works in several frequency bands requires at least two microstrip polarizable antennas. However, this will lead to some disadvantages, such as large volume, mass and high cost to the wireless systems. It will be very desirable if a single broadband CP antenna can work in the same module in multiple communication frequencies. Because it can significantly reduce the size of many wireless systems in quality, complexity and cost, broadband CP antenna has become a very hot research topic in antenna design field. Recently, there are some basic types [3]–[18] to design broadband CP antennas, such as printed slot antenna [3]–[8], printed monopole antenna [9]–[13], combined slot-monopole

antenna [14], [15], and printed dipole antenna [16]–[18]. Compared with traditional microstrip CP antennas, all the CP antennas [3]–[18] have wider impedance bandwidth and 3-dB AR bandwidth. Thus, these new types of CP antenna have a great impact on application and research prospect in many broadband communication systems.

In this paper, a simple and broadband CP antenna is designed. This antenna has a C-shaped slot and a sword-shaped radiator. An off-center feeding structure is adopted to realize wideband bandwidth. Since the radiation pattern of the antenna element is asymmetric, a 2×2 array is designed for high gain and good symmetric radiation pattern.

II. ANTENNA DESIGN AND ANALYSIS

A. CP ANTENNA ELEMENT DESIGN

Fig. 1 shows the top and side view of proposed broadband CP antenna. A square FR4 substrate material ($\epsilon_r = 4.4$, $\tan\delta = 0.02$, Dimension: $100 \times 100 \times 1.0$ mm³) is used to print this antenna. It consists of an off-center microstrip feedline, a sword-shaped microstrip radiator, and a square ground with C-shaped slot. The microstrip feedline and

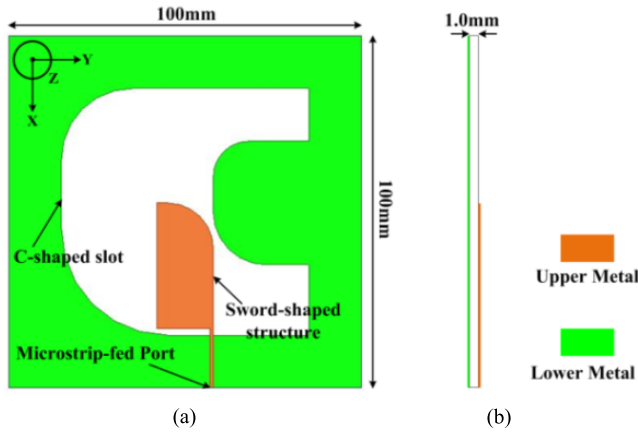


FIGURE 1. Geometry of the proposed antenna element. (a) Top view. (b) Side view.

sword-shaped radiator are printed on the top side of substrate, and the frame structure ground is printed on the lower surface. The length of the sword-shaped radiator is about $\lambda_g/4$, where λ_g is the wavelength of the antenna's operating frequency.

B. PROCESS TO REALIZE PROPOSED CP ANTENNA ELEMENT

Five steps depict the evolution structure, which is shown in Fig. 2, are used to explain the design processes of the proposed antenna. Ant. 1 only has a straight rectangular microstrip radiator and a square ground. Ant. 2 adds a metal patch on the right side of the lower ground. Ant. 3 moves the microstrip feedline along the +Y-axis ($Fd=7.5$ mm). Ant. 4 fabricates four circular chamfers ($R_1, R_2, R_3,$ and R_4) at the lower ground. Ant.5 makes the rectangular microstrip radiator to be a sword-shaped radiator with another chamfer (R_5).

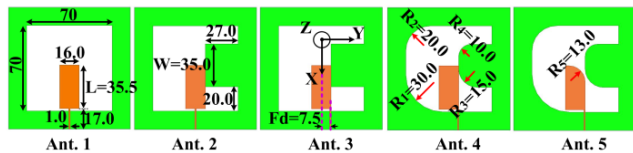


FIGURE 2. The process to design proposed CP antenna element (unit: mm).

The simulated S-parameter, amplitude ratio (E_X/E_Y), phase difference (Pd) of two orthogonal far fields E_X and E_Y in +z-direction, and axial ratio of five antennas is shown in Fig. 3. Ansoft High Frequency Structure Simulation (HFSS) software is adopted to simulate these five antennas. Ant. 1 is a simple linear polarized (LP) antenna, and the lowest working frequency is about 0.9 GHz. Ant. 2 makes the CP performance at the lower band ameliorated. However, the impedance performance is poor and the CP bandwidth is very narrow. Almost all the simulated results are improved in Ant. 3, especially at middle and upper frequencies. Ant. 4 further improves impedance matching and the Pd at middle

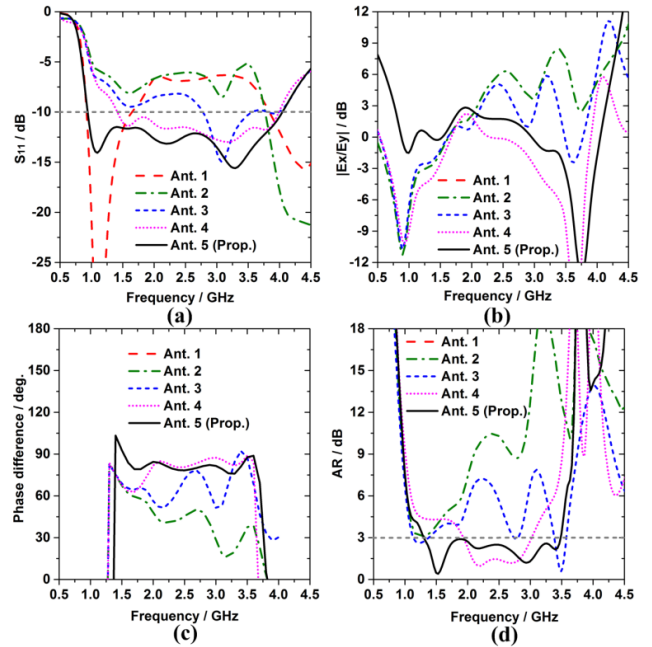


FIGURE 3. Simulated results of Ant. 1-5 (a) S_{11} , (b) E_X/E_Y , (c) Phase difference, and (d) Axial ratio.

and upper frequencies, but the amplitude ratio at lower frequency deteriorates, and this leads to a bad CP radiation. In order to solve this problem, Ant. 5 adds a chamfer (R_5) at the end of the rectangular microstrip radiator. The performance of amplitude ratio and Pd is greatly improved. Meanwhile, low frequency impedance matching is improved.

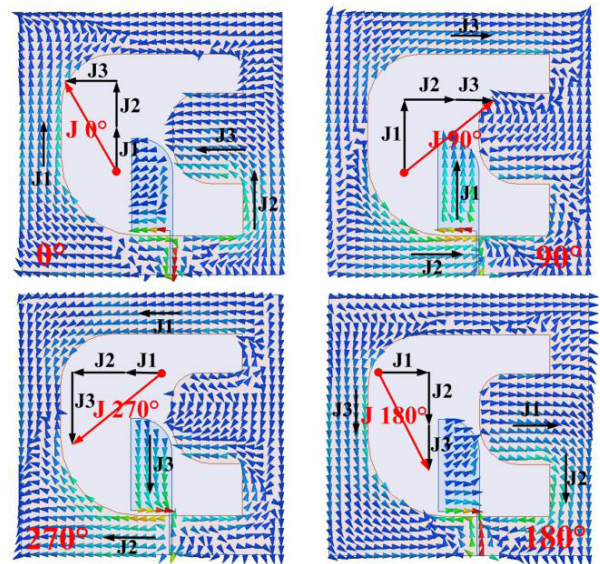


FIGURE 4. Surface current distributions of proposed antenna element at 1.5 GHz.

C. MECHANISM OF CP RADIATION

Fig. 4 shows the surface current distributions ($0^\circ, 90^\circ, 180^\circ,$ and 270°) of the proposed antenna at 1.5 and 3.0 GHz

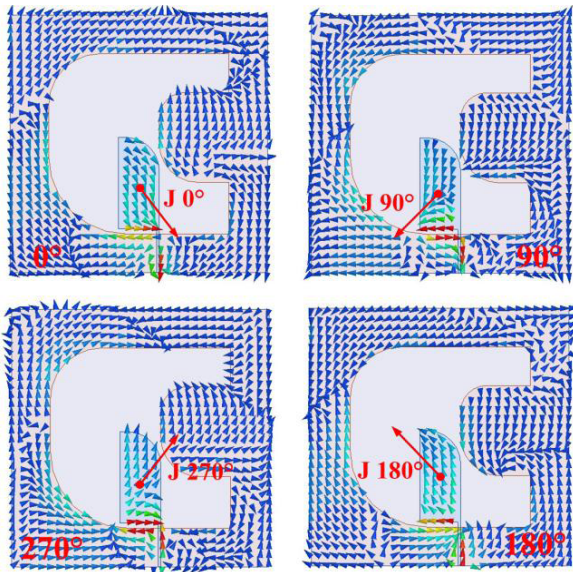


FIGURE 5. Surface current distributions of proposed antenna element at 3.0 GHz.

in Fig. 4 and Fig. 5 respectively so as to explain the generation of broadband CP radiation. It can be noticed in Fig. 4 that the 0° phase currents ($J 0^\circ$) are mainly compounded by the outer contour of C-shaped slot (J1 and J2 in $-x$ direction, and J3 in $-y$ direction). The 90° phase currents ($J 90^\circ$) are partly composed by the outer contour of C-shaped slot (J2 and J3 in $+y$ direction) and the sword-shaped radiator (J1 in $-x$ direction). The 180° phase currents ($J 180^\circ$) are mainly compounded by the outer contour of C-shaped slot (J1 in $+y$ direction, and J2, J3 in $+x$ direction). The 270° phase currents ($J 270^\circ$) are partly composed by the outer contour of C-shaped slot (J1 and J2 in $-y$ direction) and the sword-shaped radiator (J3 in $+x$ direction). As shown in Fig. 5, The CP wave at 3.0 GHz is mainly produced by the surface currents on sword-shaped radiator. The superimposed current at 0° phase is in $+x$ direction where φ is 45° . And the superimposed surface current at 90° phase is in $+x$ direction where φ is -45° . The superimposed current at 180° phase is with opposite direction of 0° phase. And the 270° phase superimposed current is in $-x$ direction where φ is 45° .

D. PARAMETERS STUDIES

Fig. 6 shows the simulated results of S_{11} and AR with the change of parameter F_d (defined in Fig. 2). As shown in Fig. 6, F_d almost has no effect on the performance of S_{11} and AR at lower frequency. However, it can broaden both impedance and CP bandwidth very well with the increase of F_d from 0.0 to 7.5 mm. When F_d is further increased to 8.0 mm, the AR value at around 1.8 GHz is greater than 3.0 dB. Therefore, an off-center microstrip-feed structure can significantly enhance the CP bandwidth, especially for the upper band. Fig. 7 shows the simulated results of S_{11} and AR with the change of R_5 . The circular chamfer (R_5) makes the rectangular microstrip radiator to be a

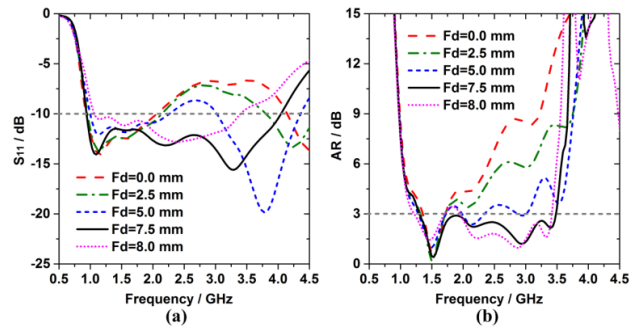


FIGURE 6. Influence of various F_d on S_{11} and AR.

sword-shaped radiator. It can provide a parameter to adjust reactance between the end of sword-shaped radiator and the C-shaped slot, and adjust the performance at lower frequency. As shown in Fig. 7, with the increase of R_5 from 0.0 to 13.0 mm, both the S_{11} and AR performance at lower frequency are gradually optimized. As it further increases to 15.0 mm, the CP performance deteriorates at around 2.0 GHz. Thus, a sword-shaped can effectually enhance the impedance and AR bandwidth, especially for the lower band.

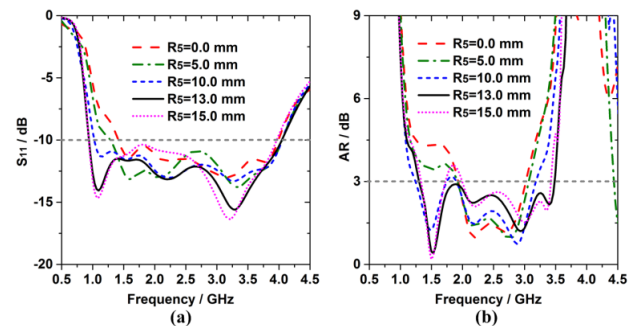


FIGURE 7. Influence of various R_5 on S_{11} and AR.

III. 2x2 ARRAY DESIGN

Since the radiation pattern of the antenna element is asymmetric for its own structure, a 2×2 array is designed for high gain and good symmetric radiation pattern in this section. As shown in Fig. 8, sequential rotation feeding scheme is used to improve the radiation pattern. The sequential rotation 2×2 antenna array is printed on square substrate 1 (FR4, size: $A \times A$) with thickness of 1.0 mm. The distance between the center of antenna element and the geometrical center of 2×2 array is D . The sequential rotation feeding network is printed on square substrate 2 ($\epsilon_r = 3.48, \tan \delta = 0.003$, size: $B \times B$) with thickness of 0.8 mm. The distance between antenna array and the feeding network is H , which is quarter wavelength at center frequency. As shown in Fig. 8 (c) a wideband coupled-line Wilkinson power divider [19] is adopted. This structure can not only feed the antenna array, but also make the antenna array to realize unidirectional radiation. The microstrip feeding structure printed on

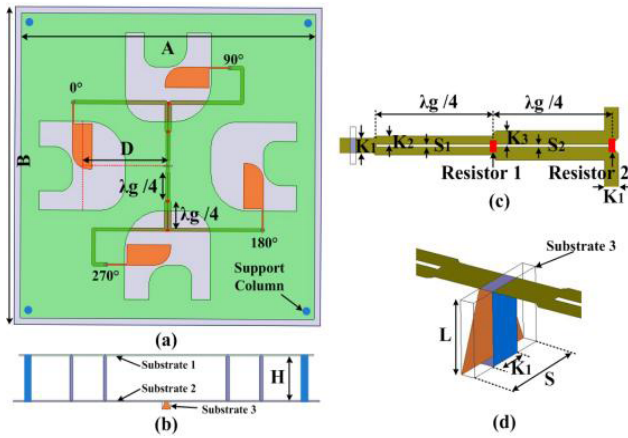


FIGURE 8. Geometry of the proposed antenna: (a) Top view, (b) Side view, (c) Wideband Wilkinson power divider, and (d) Microstrip feeding structure. $A=250$, $B=260$, $D=60$, $\lambda_g/4=23$, $H=30$, $K_1=2.7$, $K_2=1.5$, $K_3=2.5$, $S_1=0.5$, $S_2=0.5$, $L=7.0$, $S=7.0$. Unit: mm. Resistor 1=63 Ohm, Resistor 2=565 Ohm.

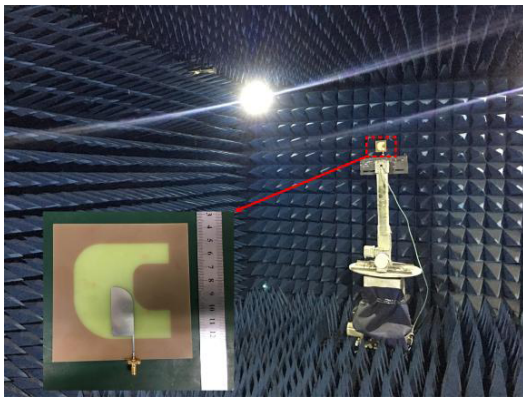


FIGURE 9. Picture of the testing antenna element in microwave anechoic chamber.

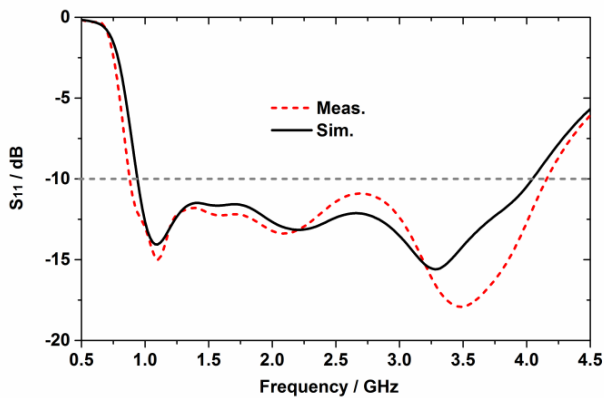


FIGURE 10. Simulated and measured S_{11} of antenna element.

substrate 3 ($\epsilon_r=2.2$, $\tan \delta = 0.0009$, size: $L \times S$) with thickness of 1.0 mm, which is shown in Fig. 8 (d), is used to generate equal power divider with out of phase.

IV. EXPERIMENTAL RESULTS

A. EXPERIMENTAL RESULTS OF ANTENNA ELEMENT

The picture of antenna element is shown in Fig. 9, and the simulated and measured S_{11} , AR and antenna gain of antenna

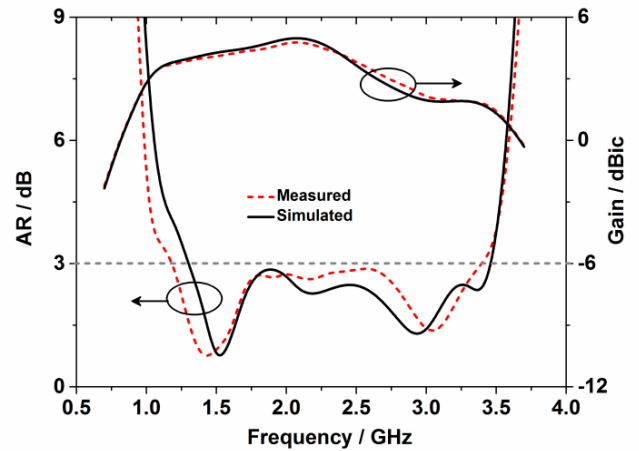


FIGURE 11. Simulated and measured AR and gain of antenna element.

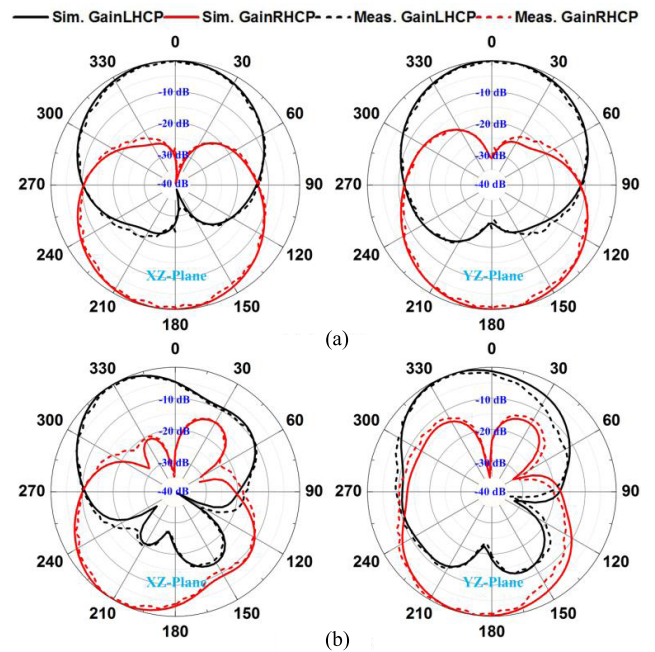


FIGURE 12. Simulated and measured normalized radiation patterns of antenna element at (a) 1.5 GHz and (b) 3.0 GHz.

element are presented in Fig. 10 and 11, respectively. The tested impedance bandwidth for $S_{11} < -10$ dB is from 0.85 to 4.15 GHz (132.0%). The measured 3-dB AR bandwidth is from 1.2 to 3.4 GHz (95.7%). The measured antenna peak gain in $+z$ direction is about 4.7 dBic at 2.0 GHz. Compared with the simulated results, the actual working frequency of fabricated antenna moves about 100 MHz to the lower frequency.

Fig. 12 shows the normalized radiation patterns of the proposed antenna element at 1.5 and 3.0 GHz in XZ-Plane and YZ-Plane. There exist about 30.0 and 26.0 dB differences between the measured LHCP and RHCP components at 1.5 and 3.0 GHz, respectively. Since the radiation patterns deviate from the $+z$ direction at 3.0 GHz, the measured

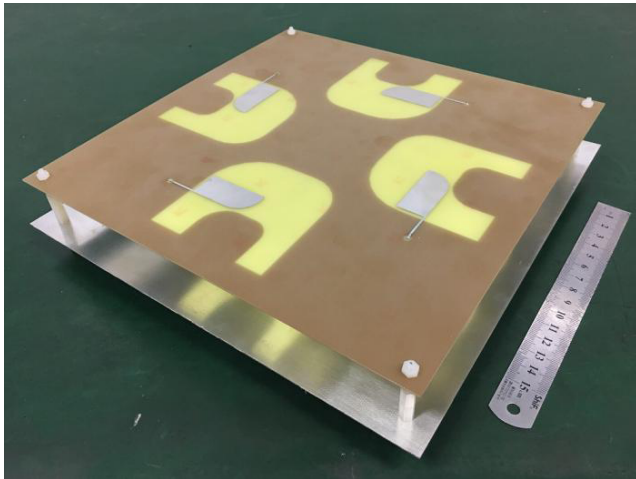


FIGURE 13. Picture of the 2 × 2 antenna array.

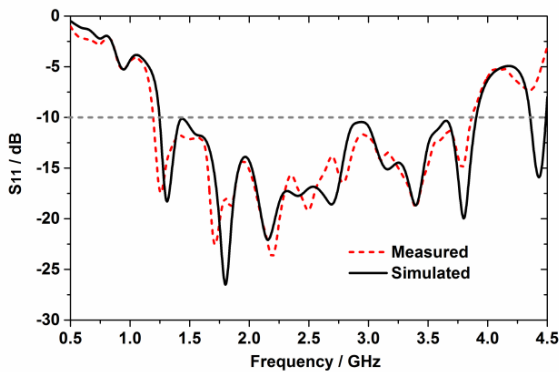


FIGURE 14. Simulated and measured S_{11} of antenna array.

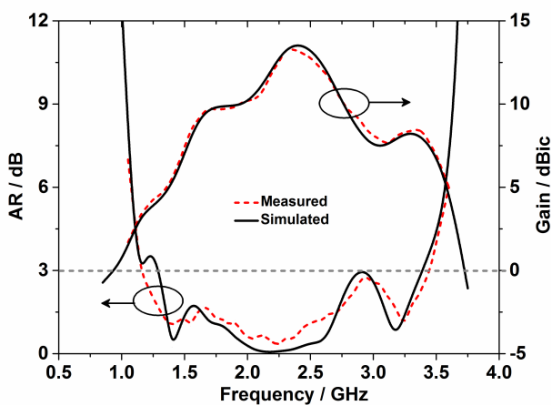


FIGURE 15. Simulated and measured AR and gain of antenna array.

antenna peak gain of the antenna element at upper band is lower than the lower band.

B. EXPERIMENTAL RESULTS OF 2×2 ANTENNA ARRAY

The fabricated antenna array is shown in Fig. 13, and the simulated and measured S_{11} , AR and antenna gain of antenna

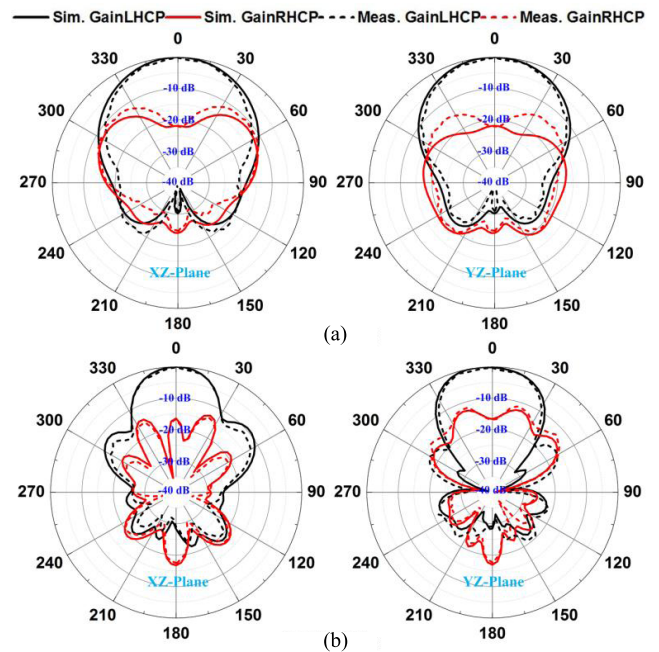


FIGURE 16. Simulated and measured normalized radiation patterns of antenna array at (a) 1.5 GHz and (b) 3.0 GHz.

TABLE 1. Comparison of broadband CP antennas.

Ref.	Size (mm ² , λ_c^2)	IBW (% , GHz)	ARBW (% , GHz)	Peak Gain (dBic)
[3]	65×65, 0.102	25.5 (1.37~1.77)	21.8 (1.47~1.83)	----
[4]	50×50, 0.283	111.0 (2.13~7.46)	27.0 (3.2~4.2)	5.3
[5]	25×25, 0.148	90.2 (3.50~9.25)	40.0 (4.6~6.9)	4.5
[6]	65×35, 0.135	56.3 (2.3~4.1)	46.7 (2.3~3.7)	3.6
[7]	20×16, 0.328	31.4 (9.2~12.5)	28.6 (9.6~12.8)	4.5
[8]	40×40, 0.40	75.0 (4.56~8.5)	41.6 (4.75~8.75)	4.4
[9]	63×58.4, 0.161	75.0 (1.5~3.3)	41.6 (1.98~3.02)	3.5
[10]	24×25, 0.134	76.9 (3.48~7.83)	44.9 (4.58~7.23)	1.9
[11]	25×25, 0.123	84.6 (4.28~10.56)	57.6 (4.2~7.6)	3.4
[12]	20×20, 0.118	40.0 (4.8~7.2)	31.8 (5.15~7.1)	3.8
[13]	100×80, 0.18	60.0 (1.4~2.6)	62.0 (1.42~2.7)	2.3
[14]	103×186, 0.768	54.9 (1.85~3.25)	34.8 (1.9~2.7)	2.3
[15]	38×54, 0.105	73.0 (1.99~4.28)	46.8 (2.13~3.43)	2.6
[16]	Φ120, 0.538	57.6 (1.88~3.4)	39.0 (2.07~3.07)	9.2
[17]	148×72, 0.266	136.0 (0.8~4.15)	77.0 (1.5~3.4)	4.2
[18]	60×40, 0.365	140.5 (1.9~10.95)	96.5 (3.7~10.6)	4.5
<i>This work (element)</i>	<i>100×100, 0.163</i>	<i>132.0 (0.85~4.15)</i>	<i>95.7 (1.20~3.4)</i>	<i>4.7</i>
<i>This work (array)</i>	<i>260×260 (H=30.0 mm)</i>	<i>108.3 (1.10~3.70)</i>	<i>100.0 (1.15~3.45)</i>	<i>13.4</i>

array are presented in Fig. 14 and 15, respectively. The measured impedance bandwidth for $S_{11} < -10$ dB is 108.3% (1.10~3.70 GHz). The measured 3-dB AR bandwidth is

about 100.0% (1.15~3.45 GHz), whereas the simulated result is 90.6% (1.28~3.40 GHz). The measured antenna peak gain reaches 13.4 dBic at 2.3 GHz.

Fig. 16 shows the normalized radiation patterns of the proposed antenna array at 1.5 and 3.0 GHz in XZ-Plane and YZ-Plane. There exist about 22.0 and 17.0 dB differences between the measured LHCP and RHCP components at 1.5 and 3.0 GHz, respectively. The radiation patterns at upper band are with good symmetry for the sequential rotation feeding scheme.

A comparison between the CP antenna element and array of this work and [3]–[18] is illustrated in Table 1, λ_L is the lowest frequency within the ARBW. It shows that the proposed antenna has simple structure, wide impedance bandwidth, and wide 3-dB AR bandwidth.

V. CONCLUSION

A broadband CP antenna with simple C-shaped square slot is designed in this paper. Both the impedance bandwidth and 3-dB AR bandwidth can be enhanced by off-center microstrip-feed sword-shaped radiator structure. A 2×2 antenna array with good symmetric radiation pattern is designed based on this broadband CP antenna element. The measured results of the antenna element exhibit an IBW of 132.0% (0.85~4.15 GHz), an ARBW of 95.7% (1.20~3.40 GHz). The Measured IBW and ARBW of the 2×2 antenna array is about 108.3% (1.10~3.70 GHz) and 100.0% (1.15~3.45 GHz), respectively. And the measured peak gain of antenna array reaches 13.4 dBic. The proposed antennas are very suitable for CP applications in L/S bands.

REFERENCES

- [1] W.-S. Chen, C.-K. Wu, and K.-L. Wong, "Novel compact circularly polarized square microstrip antenna," *IEEE Trans. Antennas Propag.*, vol. 49, no. 3, pp. 340–342, Mar. 2001.
- [2] X. Q. Nasimuddin, Y. S. Anjani, and A. Alphones, "A wide-beam circularly polarized asymmetric-microstrip antenna," *IEEE Trans. Antennas Propag.*, vol. 63, no. 8, pp. 3764–3768, Aug. 2015.
- [3] J. K. Pakkathillam and M. Kanagasabai, "Circularly polarized broadband antenna deploying fractal slot geometry," *IEEE Antennas Wireless Propag. Lett.*, vol. 14, pp. 1286–1289, 2015.
- [4] J. Y. Jan, C. Y. Pan, K. Y. Chiu, and H. M. Chen, "Broadband CPW-fed circularly-polarized slot antenna with an open slot," *IEEE Trans. Antennas Propag.*, vol. 61, no. 3, pp. 1418–1422, Mar. 2013.
- [5] M. S. Ellis, Z. Zhao, J. Wu, X. Ding, Z. Nie, and Q.-H. Liu, "A novel simple and compact microstrip-fed circularly polarized wide slot antenna with wide axial ratio bandwidth for C-band applications," *IEEE Trans. Antennas Propag.*, vol. 64, no. 4, pp. 1552–1555, Apr. 2016.
- [6] T.-N. Chang, "Wideband circularly polarised antenna using two linked annular slots," *Electron. Lett.*, vol. 47, no. 13, pp. 737–739, Jun. 2011.
- [7] J. Shen, C. Lu, W. Cao, J. Yang, and M. Li, "A novel bidirectional antenna with broadband circularly polarized radiation in X-band," *IEEE Antennas Wireless Propag. Lett.*, vol. 13, pp. 7–10, 2014.
- [8] H. Zhang, Y.-C. Jiao, L. Lu, and C. Zhang, "Broadband circularly polarized square-ring-loaded slot antenna with flat gains," *IEEE Antennas Wireless Propag. Lett.*, vol. 16, pp. 29–32, 2017.
- [9] R. C. Han and S. S. Zhong, "Broadband circularly-polarised chifre-shaped monopole antenna with asymmetric feed," *Electron. Lett.*, vol. 52, no. 4, pp. 256–258, Feb. 2016.
- [10] L. Zhang, Y.-C. Jiao, Y. Ding, B. Chen, and Z.-B. Weng, "CPW-fed broadband circularly polarized planar monopole antenna with improved ground-plane structure," *IEEE Trans. Antennas Propag.*, vol. 61, no. 9, pp. 4824–4828, Sep. 2013.

- [11] K. Ding, C. Gao, T. Yu, and D. Qu, "Broadband C-shaped circularly polarized monopole antenna," *IEEE Trans. Antennas Propag.*, vol. 63, no. 2, pp. 785–790, Feb. 2015.
- [12] S. A. Rezaeieh, A. Abbosh, and M. A. Antoniadis, "Compact CPW-fed planar monopole antenna with wide circular polarization bandwidth," *IEEE Antennas Wireless Propag. Lett.*, vol. 12, pp. 1295–1298, 2013.
- [13] A. Panahi, X. L. Bao, G. Ruvio, and M. J. Ammann, "A printed triangular monopole with wideband circular polarization," *IEEE Trans. Antennas Propag.*, vol. 63, no. 1, pp. 415–418, Jan. 2015.
- [14] T. Kumar and A. R. Harish, "Broadband circularly polarized printed slot-monopole antenna," *IEEE Antennas Wireless Propag. Lett.*, vol. 12, pp. 1531–1534, 2013.
- [15] Y.-M. Cai, K. Li, Y.-Z. Yin, and W. Hu, "Broadband circularly polarized printed antenna with branched microstrip feed," *IEEE Antennas Wireless Propag. Lett.*, vol. 13, pp. 674–677, 2014.
- [16] S.-W. Qu, C. H. Chan, and Q. Xue, "Wideband and high-gain composite cavity-backed crossed triangular bowtie dipoles for circularly polarized radiation," *IEEE Trans. Antennas Propag.*, vol. 58, no. 10, pp. 3157–3164, Oct. 2010.
- [17] K. G. Thomas and G. Praveen, "A novel wideband circularly polarized printed antenna," *IEEE Trans. Antennas Propag.*, vol. 60, no. 12, pp. 5564–5570, Dec. 2012.
- [18] R. Xu, J.-Y. Li, K. Wei, and G.-W. Yang, "Broadband rotational symmetry circularly polarized antenna," *Electron. Lett.*, vol. 52, no. 6, pp. 414–416, Feb. 2016.
- [19] Y. Wu, Y. Liu, and Q. Xue, "An analytical approach for a novel coupled-line dual-band Wilkinson power divider," *IEEE Trans. Microw. Theory Techn.*, vol. 59, no. 2, pp. 286–294, Feb. 2011.



RUI XU was born in Xi'an, China in 1989. He received the B.E. and master's degrees in electronic engineering from Northwestern Polytechnical University, Xi'an, China, in 2013 and 2015, respectively, where he is currently pursuing the Ph.D. degree in electronic engineering. His current research is in ultrawideband linear and circularly polarization antennas, waveguide slot antenna arrays, print slot antennas, microstrip antennas, and electromagnetic periodic structure.



JIAN-YING LI received the B.Sc. degree in mathematics from Henan Normal University, Xinxiang, China, in 1986, and the M.Eng.Sc. and Ph.D. degrees in electromagnetic field and microwave technology from Xidian University, Xi'an, China, in 1992 and 1999, respectively. From 1999 to 2004, he was a Post-Doctoral Research Fellow with the Department of Electrical and Computer Engineering, National University of Singapore, and then a Research Fellow with High Performance Computation for Engineered Systems Programme, Singapore-MIT Alliance. From 2005 to 2010, he was with Temasek Laboratories, National University of Singapore. Since 2011, he has been with School of Electronic and Information, Northwestern Polytechnical University. His current research interests include the fast algorithms and its applications to radar cross sections, analysis and design of phased arrays, waveguide slot antennas and microstrip antennas, and electromagnetic periodic structure.



JIE LIU received the B.Sc. degree in electronic engineering from Northwestern Polytechnical University in 2013, where she is currently pursuing the Ph.D. degree in electronic engineering. Her current research is in reconfigurable antennas, slot antennas, and electromagnetic periodic structure.